Published OnlineFirst May 21, 2013; DOI: 10.1158/0008-5472.CAN-12-4539

VEGF-C and VEGF-D Blockade Inhibits Inflammatory Skin Carcinogenesis

Annamari K. Alitalo[1], Steven T. Proulx[1], Sinem Karaman[1], David Aebischer[1], Stefania Martino[1], Manuela Jost[1], Nicole Schneider[1], Maija Bry[2], and Michael Detmar[1]

Abstract

VEGF-C and VEGF-D were identified as lymphangiogenic growth factors and later shown to promote tumor metastasis, but their effects on carcinogenesis are poorly understood. Here, we have studied the effects of VEGF-C and VEGF-D on tumor development in the murine multistep chemical carcinogenesis model of squamous cell carcinoma by using a soluble VEGF-C/VEGF-D inhibitor. After topical treatment with a tumor initiator and repeated tumor promoter applications, transgenic mice expressing a soluble VEGF-C/VEGF-D receptor (sVEGFR-3) in the skin developed significantly fewer squamous cell tumors with a delayed onset when compared with wild-type mice or mice expressing sVEGFR-3 lacking the ligand-binding site. Epidermal proliferation was reduced in the carcinogen-treated transgenic skin, whereas epidermal keratinocyte proliferation *in vitro* was not affected by VEGF-C or VEGF-D, indicating indirect effects of sVEGFR-3 expression. Importantly, transgenic mouse skin was less sensitive to tumor promoter–induced inflammation, with reduced angiogenesis and blood vessel leakage. Cutaneous leukocytes, especially macrophages, were reduced in transgenic skin without major changes in macrophage polarization or blood monocyte numbers. Several macrophage-associated cytokines were also reduced in transgenic papillomas, although the dermal macrophages themselves did not express VEGFR-3. These findings indicate that VEGF-C/VEGF-D are involved in shaping the inflammatory tumor microenvironment that regulates early tumor progression. Our results support the use of VEGF-C/VEGF-D–blocking agents not only to inhibit metastatic progression, but also during the early stages of tumor growth. *Cancer Res; 73(14); 1–10. ©2013 AACR.*

Introduction

Nonmelanoma skin cancer (NMSC) is the most common human cancer. The basal cell carcinoma and squamous cell carcinoma (SCC) subtypes constitute the majority of NMSCs. High-risk populations for the development of NMSC can be identified and may benefit from preventive strategies.

Although angiogenesis is required for the progression of solid tumors beyond a critical size, the role of lymphatic vessels in primary tumor growth has not been studied in detail. VEGF-C and VEGF-D activate VEGF receptor 3 (VEGFR-3) signaling that is critical for the growth of lymphatic vessels, a process known as lymphangiogenesis (1, 2). Besides constitutive expression on lymphatic vessels, VEGFR-3 is also expressed in angiogenic blood vessel sprouts (3). Thus, VEGFR-3 signaling may also modulate the growth of blood vessels (angiogenesis). Indeed, inhibition of ligand-induced VEGFR-3 signaling was found to reduce angiogenesis in some tumor types, with a stronger effect when combined with VEGFR-2 inhibition (4). In its proteolytically processed form, the VEGFR-3 ligand VEGF-C can also activate VEGFR-2, although less potently than the strongly angiogenic VEGF-A. In contrast, the mouse VEGF-D does not activate VEGFR-2 (5).

In a previous study, high VEGF-C expression in SCC led to enhanced tumor lymphangiogenesis and metastasis but did not affect tumor incidence; possible effects on tumor growth rate were not studied (6). In contrast, antibody-mediated VEGFR-3 blockage was reported to decrease the growth rate of several transplanted carcinomas (7, 8). For tumor growth, a permissive tissue microenvironment is required. Inflammation and angiogenic factors derived from tissue infiltrating inflammatory cells act to promote tumor growth (9). Tumor-associated macrophages may polarize toward antitumor immune responses or protumor functions such as the production of VEGF-A. A role for VEGFR-3 activation in promoting the recruitment of proangiogenic tissue macrophages was previously suggested in a subcutaneously growing mouse melanoma model (10, 11).

In this study, we investigated the effects of the expression of a soluble form of VEGFR-3 (sVEGFR-3) on the development of chemically induced squamous cell tumors in mouse skin. SVEGFR-3, consisting of domains 1 to 3 of human VEGFR-3 fused to the Fc-part of human IgG, was expressed under the

Authors' Affiliations: [1]Institute of Pharmaceutical Sciences, Swiss Federal Institute of Technology, ETH Zurich, Zurich, Switzerland; and [2]Translational Cancer Biology Program, Biomedicum Helsinki, Helsinki, Finland

Note: Supplementary data for this article are available at Cancer Research Online (http://cancerres.aacrjournals.org/).

Corresponding Author: Michael Detmar, Institute of Pharmaceutical Sciences, Swiss Federal Institute of Technology, ETH Zurich, Wolfgang Pauli-Str. 10, HCI H303, CH-8093 Zurich, Switzerland. Phone: 41-44-633-7361; Fax: 41-44-633-1364; E-mail: michael.detmar@pharma.ethz.ch

doi: 10.1158/0008-5472.CAN-12-4539

Published OnlineFirst May 21, 2013; DOI: 10.1158/0008-5472.CAN-12-4539

keratin 14 (K14) promoter in the skin of transgenic mice (12). These transgenic mice lack cutaneous lymphatic vessels but a normal blood vasculature has been previously described in these mice (12). We used a two-step chemical carcinogenesis model of SCC (13) to study the effects of VEGFR-3 ligand blockage on early tumor initiation and growth. As in this model tumors develop after 10 weeks of treatment, long-term VEGF-C and VEGF-D blockade was implemented through constitutive transgenic expression of sVEGFR-3.

Surprisingly, we found that squamous tumor development was significantly reduced in sVEGFR-3 transgenic mice. Several aspects of the tumor microenvironment, in particular the levels of pro-inflammatory mediators, were also found altered by the blockage of VEGF-C/VEGF-D. By studying early tumor growth, we found that although VEGFR-3 expression was restricted to lymphatic vessels, VEGFR-3 ligand inhibition reduced tumor incidence via diverse effects on angiogenesis, blood vascular leakage, and the inflammatory tissue microenvironment. Together, these findings indicate a potential of VEGFR-3 inhibition in cancer chemoprevention and therapy.

Materials and Methods

Transgenic mice

All mouse experiments were approved by the Veterinäramt of the Kanton Zurich. K14-VEGFR-3 domain 1 to 3—Fc transgenic mice [FvB-TgN(K14-VEGFR-3d1-3-Fc)] express a sVEGFR-3 in the basal epidermal keratinocytes of the skin (12). K14-VEGFR-3 domain 4 to 7—Fc transgenic [FvB-TgN(K14-VEGFR-3d4-7-Fc), referred to here as "control transgenic"] mice were generated similarly. Hemizygous transgenic but not control transgenic mice show a phenotype of mild edema of the legs (paws), tail, and snout.

Chemical carcinogenesis

An established multistep chemical carcinogenesis protocol was followed to induce SCCs of the skin (13). Female wild-type FvB-strain mice were shaved on their back skin in isoflurane anesthesia at 8 weeks of age. Two days later, mutations in DNA were induced by topical application of 50 μg of the tumor initiator 7,12-dimethylbenz(a)anthracene (DMBA) in acetone (200 μL) on the back skin of mice anesthetized with ketamine–medetomidine. Subsequently, 5 μg of the promoter 12-O-tetradecanoyl-phorbol-13-acetate (TPA) in 200 μL acetone was applied once per week on the back skin of mice anesthetized with ketamine–medetomidine. The mice were shaved under isoflurane anesthesia 2 days before TPA treatment. In a first long-term study, tumor growth and malignant transformation were observed in 35 transgenic and 35 wild-type mice. Tumors were scored weekly in a blinded manner and mice were sacrificed by overdose of anesthetic 6 weeks after SCC development. Skin samples from the carcinogen treatment area (back) and untreated control area (abdomen), papillomas, carcinomas, and serum were collected. Short-term DMBA-TPA treatment (DMBA followed by 5, 14, or 15 weekly TPA treatments) was used to study tumor initiation, inflammation, and early tumor growth. Blood vascular leakage was imaged non-invasively (as described later) 24 to 30 hours after 3 or 14 TPA treatments. The mice were sacrificed overdose of anesthetics 48 to 52 hours after the last TPA treatment and the treated back skin was collected. For gene expression analyses, macrophages were isolated by fluorescence-assisted cell sorting (FACS) from the treated back skin (as described in Supplementary Methods) 24 hours after the fifth TPA treatment. TPA-treated back skin was also collected 6 hours after 14 weekly TPA treatments for analysis of TNF-α levels. To further investigate vascular leakage, inflammation was induced in ear skin by application of 0.5 μg TPA (in 20 μL acetone) weekly on one ear under ketamine–medetomidine anesthesia. The other ear was left as an untreated control. VEGFR-3, CD68, CD11b, MECA32, and podoplanin were immunostained in ears collected 48 hours after single TPA treatment and in untreated ears.

Immunofluorescence staining of tissue sections

Tissue cryosections were blocked using immunomix (5% nonimmune donkey serum, 0.2% bovine serum albumin (BSA), and 0.05% NaN_3 in PBS with 0.3% Triton X) or antibody diluent (Zytomed). Primary antibodies and analyses are described in Supplementary Methods. AlexaFluor conjugated secondary antibodies (Invitrogen) and Hoechst 33342 (Invitrogen) nuclear stain were used.

Measurement of blood vascular leakage

Vascular leakage was quantified by dynamic imaging using an IVIS Sprectrum (Caliper Life Sciences) after a tail vein injection of a pegylated near-infrared dye to anesthetized mice (14). A detailed description of the method is given in the Supplementary Methods.

Statistical analyses

A two-tailed Student *t* test was used for comparisons of continuous variables between two groups. For comparisons between three groups, one-way ANOVA with Tukey or Dunnett posttest was used. For comparison of tumor incidences, the two-tailed Fisher exact test was used.

Results

Reduced tumor development in sVEGFR-3 transgenic mice

A previously described chemical carcinogenesis protocol was used to generate tumors in wild-type and in K14-VEGFR-3 transgenic mice (13). Serum concentrations of the sVEGFR-3 protein were 17 ± 11 ng/mL in untreated transgenic mice, whereas a strong upregulation was found after 21 weeks of DMBA-TPA treatment (309 ± 60 ng/mL; Supplementary Fig. S1A), due to activation of the K14 promoter in the hyperplastic epidermis. The untreated dermis of transgenic mice was significantly thicker than that of wild-type littermates (406 ± 25 μm vs. 270 ± 36 μm, respectively, $P = 0.006$), whereas no major differences in epidermal thickness were found (Fig. 1A). In contrast, the epidermis of transgenic mice was significantly thinner than that of wild-type mice after 21 weeks of the DMBA-TPA treatment (19 ± 2.5 μm vs. 26 ± 4.7 μm, respectively, $P = 0.04$; Fig. 1A).

Tumor growth was scored weekly, and over 1-mm-diameter tumors were counted. Morphologically heterogeneous, aggressive, and infiltrative tumors over 5 mm in diameter were scored

Published OnlineFirst May 21, 2013; DOI: 10.1158/0008-5472.CAN-12-4539

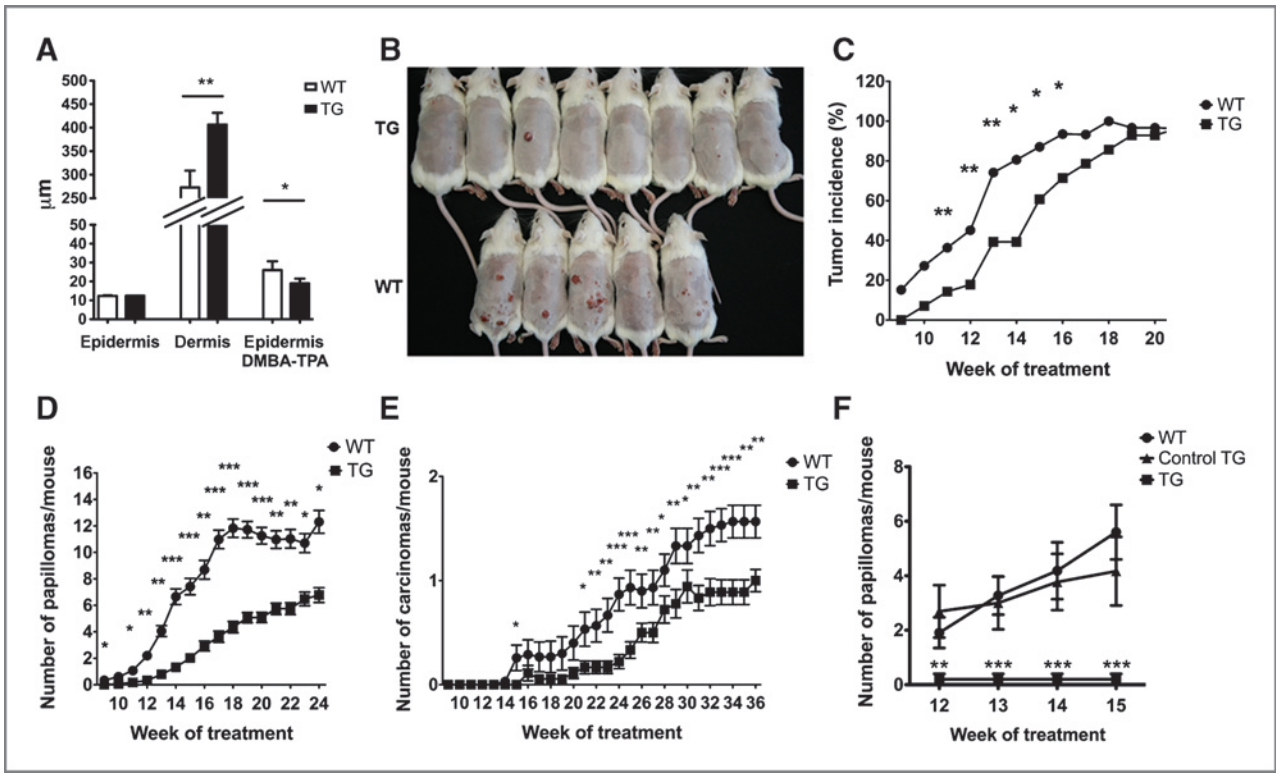

Figure 1. Epidermal hyperplasia and tumor development in transgenic and wild-type mice in response to chemical carcinogenesis treatment. A, epidermal and dermal thickness in wild-type and transgenic mice ($n = 3$–4). B, shaved transgenic and wild-type mice after 14 weeks of DMBA-TPA treatment. C, tumor incidence ($n = 28$). D, number of papillomas per mouse in transgenic and wild-type mice per week of DMBA-TPA treatment ($n = 28$). E, number of carcinomas in long-term follow up ($n = 28$). F, number of papillomas in transgenic, control transgenic, and wild-type mice per mouse per week of DMBA-TPA treatment ($n = 10$–14). WT, wild-type; TG, transgenic; *, $P < 0.05$; **, $P < 0.01$; ***, $P < 0.001$.

as SCC. Surprisingly, tumor incidence, that is the proportion of mice bearing at least one tumor, was significantly smaller in the transgenic mice and they developed significantly fewer papillomas per mouse when compared with the wild-type mice (Fig. 1B–D). The growth rates of established tumors did not differ significantly between the wild-type and transgenic mice and the malignant conversion rate was unaffected (Fig. 1E; Supplementary Fig. S1B and S1C). To investigate the possibility that the smaller tumor incidence in transgenic mice was caused by the Fc-part of the sVEGFR-3 fusion protein, we generated another transgenic mouse line (called control transgenic from here on). These mice express a sVEGFR-3 protein where the VEGF-C/VEGF-D binding domains 1 to 3 have been replaced by domains 4 to 7 that are not involved in ligand binding. Control transgenic mice showed no apparent phenotype, their cutaneous lymphatic vasculature seemed normal in immunofluorescence stainings (data not shown), and SCC growth was similar to that of wild-type mice (Fig. 1F).

Because of the delayed incidence and reduced tumor growth in the transgenic mice expressing the VEGF-C and VEGF-D inhibitor, we next investigated whether VEGF-C or VEGF-D exerts direct effects on the survival and proliferation of epidermal keratinocytes. EGF stimulated the proliferation of cultured keratinocytes, whereas VEGF-C, VEGF-D, or BSA did not have any significant effects (Supplementary Fig. S1D). We thus considered it unlikely that the blockage of VEGF-C and VEGF-D by sVEGFR-3 would directly inhibit tumor cell proliferation in transgenic mice.

Attenuated angiogenesis in DMBA-TPA–treated skin and tumors of K14-VEGFR-3 transgenic mice

Previous studies have shown that the chemical carcinogenesis treatment activates angiogenesis in the skin (6, 15). To study the effects of sVEGFR-3 on angiogenesis, blood vessel areas were quantified by immunofluorescence staining for the endothelial markers MECA32 and CD31. Compared with wild-type mice, the blood vessel area was slightly smaller in the back skin and in tumors of transgenic mice (Fig. 2A). After DMBA and 14 weekly TPA applications, the blood vessel density in the skin of transgenic mice was significantly lower than in the treated skin of wild-type mice (Fig. 2B). In tumor-bearing mice (21 weeks of treatment, followed by an average period of 10 weeks), the blood vessel density was also lower in the TPA-treated skin of transgenic mice than in wild-type mice, although the differences did not reach statistical significance (Fig. 2C). The intratumoral blood vessel density was variable due to the highly heterogeneous morphology typical of squamous cell tumors. The trend toward smaller vessel density in papillomas and SCCs of transgenic mice was statistically significant when the data for papillomas and carcinomas were combined (transgenic 2.5 ± 1.7 vs. wild-type 4.3 ± 2.4 area percentage, $P = 0.01$; Fig. 2C).

Published OnlineFirst May 21, 2013; DOI: 10.1158/0008-5472.CAN-12-4539

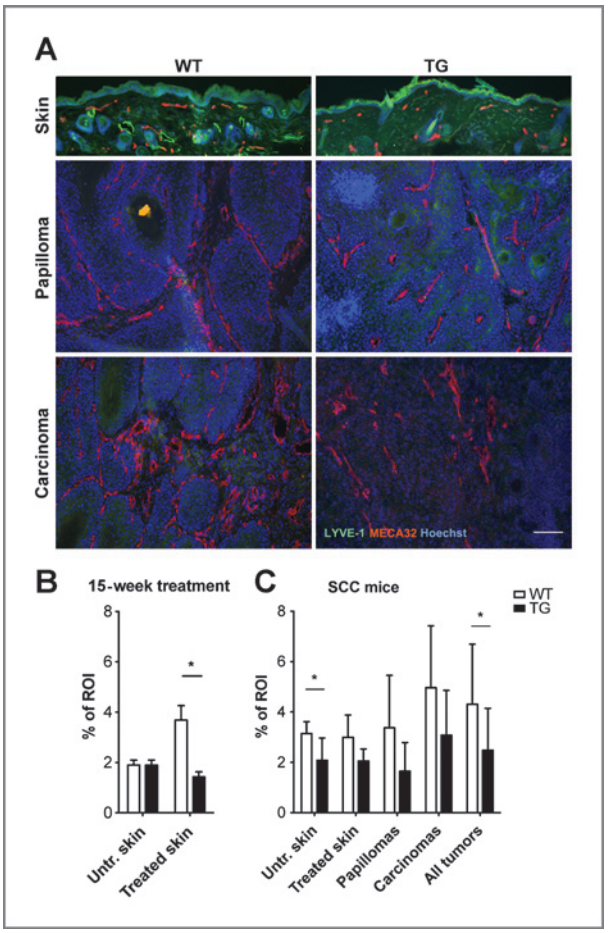

Figure 2. Blood vessel density in skin and cutaneous tumors. A, immunofluorescence staining of blood (MECA32; red) and lymphatic (LYVE-1; green) vessels in DMBA-TPA–treated skin, papillomas, and carcinomas of transgenic and wild-type mice. Note the absence of lymphatic vessels in transgenic skin. Intratumoral areas lack lymphatic vessels in transgenic and wild-type mice. Scale bar, 100 μm. B, quantification of blood vessel area in untreated abdominal skin and treated back skin of transgenic and wild-type mice. Note that the blood vessel area was significantly reduced in the back skin of transgenic mice, compared with the wild-type mice, after 15-week treatment (DMBA plus 14 weeks of TPA, $n = 5$). C, quantification of blood vessel area in untreated abdominal skin, DMBA-TPA (21-week)–treated back skin, papillomas, carcinomas, and all tumors of mice bearing SCCs ($n = 7$–19). Note a trend toward reduced blood vessel area in all transgenic samples. ROI, region of interest; the dermis, excluding hair follicles, in skin and intratumoral area in tumor sections. *, $P < 0.05$.

Less DMBA-TPA–induced skin inflammation in K14-VEGFR-3 transgenic mice

A striking difference was observed in the degree of cutaneous inflammation between transgenic and wild-type mice at 4 weeks of DMBA-TPA treatment (Fig. 3A). The wild-type mice displayed pronounced scaling and redness of the shaved skin, whereas transgenic mice showed only little redness and a few hairless patches. We therefore next analyzed blood vascular leakage, leukocyte recruitment, and inflammatory cytokines in the treated skin of transgenic and wild-type mice.

Blood vessel permeability is increased under inflammatory conditions and in tumors. Dynamic assessments of vascular leakage were made using a pegylated near-infrared dye injected intravenously. We first measured vascular leakage in untreated and TPA-treated ears for easy comparison of anatomically identical areas of the skin, thus providing a better identification of changes caused by the treatment. Significantly less leakage of the tracer was found in the untreated ears of transgenic mice than in wild-type mice ($P = 0.0063$; Fig. 3B). After three weekly TPA treatments, strongly increased leakage rates were detected in the ears of wild-type mice ($P = 0.0003$; Fig. 3B). In contrast, the leakage of the tracer was significantly lower in treated transgenic mice ($P < 0.0001$). Lower leakage rates were also observed in the back skin of transgenic mice when compared with wild-type mice ($P = 0.0002$ and 0.0058 after 3 and 14 TPA treatments, respectively).

Reduced macrophage recruitment in the skin of K14-VEGFR-3 transgenic mice

Cutaneous inflammation involves recruitment of inflammatory cells to the skin. Markedly, fewer $CD45^+$ leukocytes were observed in the untreated and DMBA-TPA treated skin of transgenic mice when compared with wild-type mice ($P = 0.006$ and 0.06, respectively; Fig. 4A and B). Leukocyte densities in papillomas of transgenic mice were also somewhat less than in papillomas of wild-type mice whereas no major differences were found in SCCs.

To further characterize the leukocyte infiltrates, the skin and tumor sections were stained using the leukocyte markers CD11b (monocytes, granulocytes, macrophages, and mast cells), F4/80 (M2 macrophages, eosinophils), and CD68 (macrophages). $CD11b^+$ leukocytes were significantly less abundant in untreated abdominal skin and treated back skin (both $P < 0.05$) of transgenic mice than in wild-type mice (Fig. 5A and B). The CD11b leukocyte counts were decreased in transgenic papillomas and carcinomas when compared with DMBA-TPA–treated transgenic skin; however such trend was not found in wild-type mice. Thus, the density of $CD11b^+$ cells was significantly lower in the SCCs of transgenic mice than of wild-type mice ($P = 0.04$; Fig. 5B). The $F4/80^+$ cells could not be reliably counted as individual cells, but the tissue area % stained for F4/80 was smaller in untreated abdominal skin and treated back skin of transgenic mice ($P = 0.054$ and 0.0019, respectively; Fig. 5C). In the dermis, high CD68 expression is restricted to macrophages whereas dendritic cells express lower levels of this marker (16). Staining untreated and treated skin for CD68 confirmed that there were fewer macrophages in transgenic skin ($P = 0.0012$ and 0.0078, respectively; Fig. 5D).

There were fewer $CD68^+$ cells in the DMBA-TPA–treated back skin (6 weeks of treatment) of transgenic mice than in control transgenic mice or wild-type mice ($P < 0.05$; Fig. 5E). Therefore, the low cutaneous $CD68^+$ cell counts in the transgenic mice were specifically associated with the blockage of VEGF-C and VEGF-D. Accordingly, lower levels of TNF-α, an important proinflammatory cytokine secreted by macrophages, were detected in the DMBA-TPA–treated skin

Published OnlineFirst May 21, 2013; DOI: 10.1158/0008-5472.CAN-12-4539

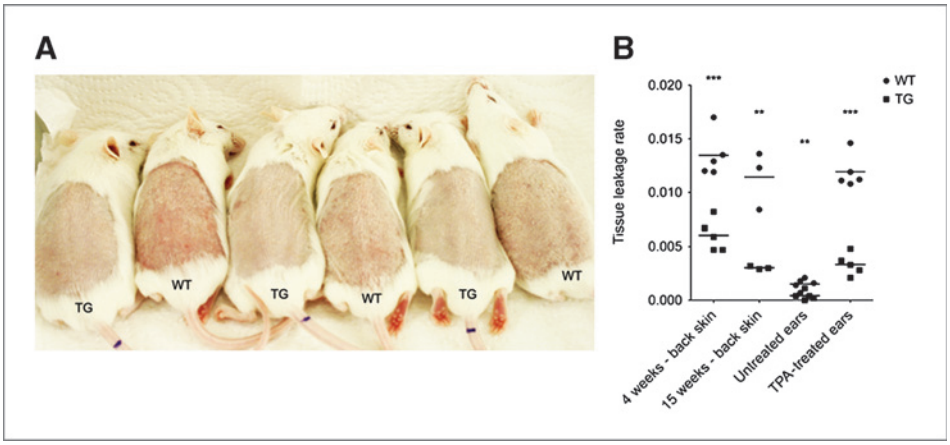

Figure 3. SVEGFR-3 transgenic mice have less cutaneous inflammation and vascular leakage after DMBA-TPA treatment. A, inflammatory changes in the shaved back skin of wild-type and transgenic mice after 4 weeks of DMBA-TPA treatment. B, blood vessel leakage in TPA-treated back skin and in untreated and treated ears. Highly significantly reduced leakage rates in inflamed skin of transgenic mice compared with wild-type mice. Four weeks treatment: one DMBA and three TPA applications; 15 weeks treatment: one DMBA and 14 TPA applications. TPA-treated ears: three TPA applications. **, $P < 0.01$; ***, $P < 0.001$.

of transgenic mice than in wild-type or control transgenic mice ($P < 0.01$; Fig. 5F). The relative blood leukocyte or monocyte counts in wild-type and transgenic mice did not differ significantly ($P = 0.11$ and 0.63, respectively; Supplementary Fig. S2).

We next quantified T-cell populations in DMBA-TPA–treated skin because a deficiency of $CD4^+$ helper T cells has previously been reported to attenuate tumor development in human papilloma virus gene 16 transgenic mice, whereas a deficiency of $CD8^+$ cytotoxic cells had less influence on tumor development, possibly delaying tumor growth (17). Significantly fewer $CD4^+$ and $CD8^+$ cells were found in the DMBA-TPA–treated transgenic skin compared with similarly treated wild-type and control transgenic skin (Fig. 6A; Supplementary Fig. S3). These results were confirmed by flow cytometric analysis of the cells (Fig. 6B).

Macrophage M1/M2 polarization is not altered by the K14-VEGFR-3 transgene

The tumor microenvironment has profound effects on the "polarization" of tumor-associated macrophages to antitumor (M1 or classically activated) or protumor (M2 or alternatively activated) effector cells. M1 macrophages secrete the antiangiogenic interleukins (IL)-12 and IL-23, kill microorganisms and tumor cells, and present antigens, efficiently activating antitumor immunity, whereas M2 macrophages potentiate tissue remodeling, secrete VEGF-A and MMP-9 and thereby activate angiogenesis and facilitate tumor metastasis (18). We analyzed cutaneous cytokine levels to characterize the polarization of the immune system and angiogenic signaling in the tumor microenvironment of DMBA-TPA–treated skin and tumors. Several macrophage-associated cytokines were selected on the basis of preliminary screening using cytokine arrays and many of these cytokines were found at lower levels in the papillomas of transgenic mice (Supplementary Table S1). Lower levels were also observed for MCP-1 (CCL2), MIP-1α, and IL-16. To address possible differences in the pro- or antitumor polarization of the tumor microenvironment, VEGF-A, IL-12 (p40), IL-4, IL-6, and IL-10 were quantified in the skin of mice treated for 14 weeks. No major differences were found except for the antiangiogenic M1 cytokine IL-12 that was detected at higher levels in the transgenic than wild-type skin.

Next, macrophage polarization was analyzed by cell surface marker expression on $CD45^+$, $CD11b^+$ cells, and in RNA isolated from $CD45^+$, $CD11b^+$, $F4/80^+$ positive cells obtained from the back skin of mice treated with DMBA-TPA for 5 weeks (Supplementary Fig. S4). The percentage of macrophages expressing the M2 surface markers Tie2 and CD206 was similar in transgenic and wild-type skin. However, macrophages from transgenic skin expressed lower levels of the M2 "angiogenic" macrophage marker Tie2 (Supplementary Fig. S4A and S4B). No significant differences were observed in the levels of *Vegf*, *Lyve-1*, *Tnfa*, *Il-10*, or *Tie2* mRNAs (Supplementary Fig. S4C). Thus, we conclude that the polarization of cutaneous macrophages does not differ between transgenic and wild-type mice.

Hypothetically, the decreased macrophage density in the skin of transgenic mice could be explained by blockage of possible chemotactic effects of VEGF-C and/or VEGF-D on VEGFR-3 expressing macrophages (10, 11). However, in double staining for the macrophage markers CD11b and CD68 with VEGFR-3, no VEGFR-3 expression was observed in cutaneous macrophages in untreated or DMBA-TPA–treated skin or SCCs (Fig. 7; Supplementary Fig. S5). Furthermore, *Vegfr3* mRNA levels were below the detection limit in isolated skin-derived macrophages (data not shown). VEGFR-3 expression was not observed in blood vessels 48 hours after a single TPA treatment but VEGFR-3 was expressed in cutaneous blood vessels after long-term DMBA-TPA and on some peritumoral blood vessels (Supplementary Fig. S5).

The expression of the VEGF coreceptors neuropilins (Nrp) was analyzed next. Expression of Nrp-2 was observed in vascular endothelium and in the epidermis (Supplementary

Published OnlineFirst May 21, 2013; DOI: 10.1158/0008-5472.CAN-12-4539

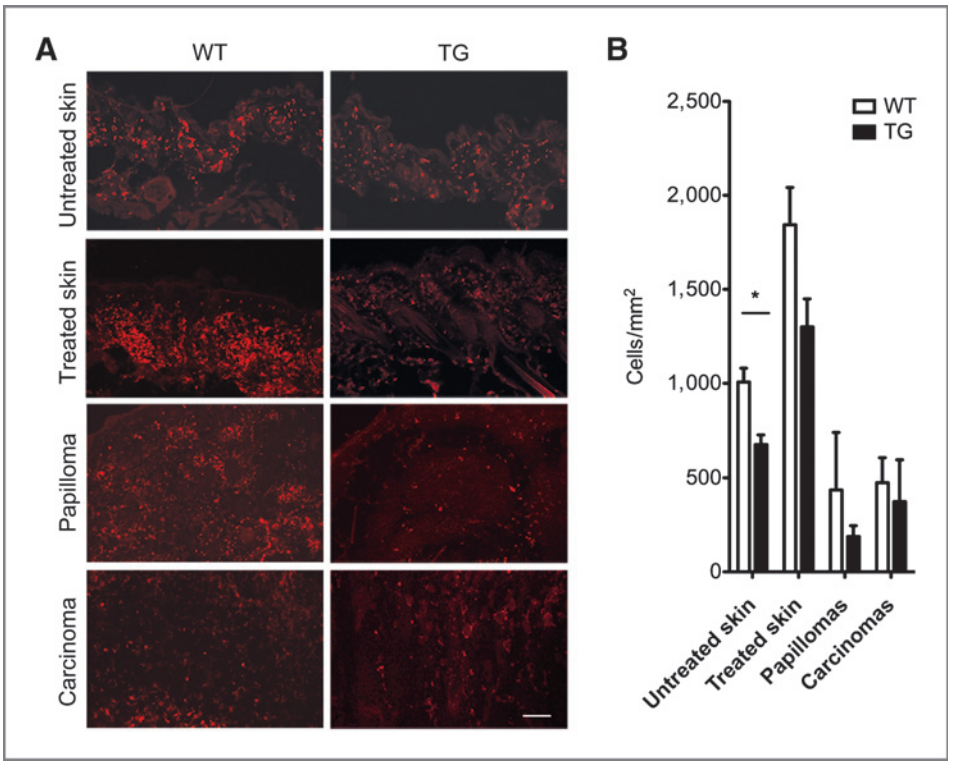

Figure 4. Analysis of leukocyte numbers in wild-type and transgenic skin and tumors. A, representative images of sections stained with antibodies against CD45 (red). Scale bar, 100 μm. B, quantification of $CD45^+$ cells/mm^2 of dermal or tumor section. $n = 4–5$; *, $P < 0.05$.

Fig. S6). Nrp-1 was expressed in the epidermis, on blood vessels in the dermis, and in the tumor interstitium. CD68-expressing cutaneous macrophages did not express Nrp-1 or Nrp-2 in untreated or DMBA-TPA–treated skin or tumors.

Discussion

In this study, we show that transgenic VEGFR-3 ligand blockage decreases the development and growth of cutaneous papillomas and SCCs in a mouse chemical carcinogenesis model. Importantly, VEGF-C or VEGF-D did not exert direct effects on the proliferation of isolated epidermal cells. This is in line with previous results showing that high expression of VEGF-C in the epidermis of transgenic mice did not promote skin carcinogenesis (6). However, VEGF-C and VEGF-D blockage influenced the vascular and inflammatory tissue microenvironment that is required for efficient tumor development, pinpointing to novel effects of VEGF-C and/or VEGF-D on critical components of the tumor microenvironment in the chemically induced SCC model.

We found that the density of blood vessels was reduced in the skin and in tumors of transgenic mice in which VEGF-C and VEGF-D were blocked. This is consistent with the finding that VEGFR-3 may provide angiogenic signals when expressed in blood vessel endothelium (4, 19). Activation of angiogenesis facilitates tumor growth by provision of oxygen and nutrients, whereas activation of lymphangiogenesis facilitates tumor dissemination (1). Angiogenesis and lymphangiogenesis are induced in human cutaneous SCCs (20, 21). This is accompanied by increased expression of genes associated with lymphangiogenesis, such as VEGF-C, Nrp-2, and VEGFR-3, in peritumoral skin (20). However, in contrast to blood vessels, lymphatic vessels are not known to directly affect primary tumor growth. The observed blood vascular effects of sVEGFR-3 may be explained by inhibition of VEGF-C–induced VEGFR-2 activation, and VEGFR-2/VEGFR-3 heterodimers in blood vascular endothelium (22). Blood vascular VEGFR-3 expression was detected in long-term DMBA-TPA–treated skin and in tumors but not in untreated skin or TPA-promoted skin. Therefore, the observed reduction of angiogenesis in the skin of the transgenic mice may be mediated mainly through inhibition of VEGF-C/VEGFR-2 interactions, in particular as mouse VEGF-D does not bind to mouse VEGFR-2 (5).

VEGFR-3 ligand blockage also potently reduced inflammation, which is thought to be mediated mainly by VEGFR-3–independent angiogenic signaling via VEGF-A produced by macrophages. Although blood vascular VEGFR-3 expression was not observed in the untreated skin, the transgenic mice showed reduced blood vascular leakage that was increased after the DMBA-TPA treatment. Indeed, high expression levels of VEGF-C may increase blood vascular permeability, most likely via VEGFR-2 signaling (23, 24). Importantly, however, the lack of lymphatic vessels increases interstitial pressure in transgenic mice (25), which can counteract blood vascular leakage. This is likely to restrict the extravasation of inflammatory mediators reducing, for example invasion of inflammatory cells, and other tumor-promoting molecules such as fibrinogen (26).

Under physiological conditions, lymphatic vessels transport fluid, soluble factors, and cells to the lymph nodes. Antigen presenting cells (APC, such as activated dendritic cells from the skin) travel through the lymphatic vessels to the draining

Published OnlineFirst May 21, 2013; DOI: 10.1158/0008-5472.CAN-12-4539

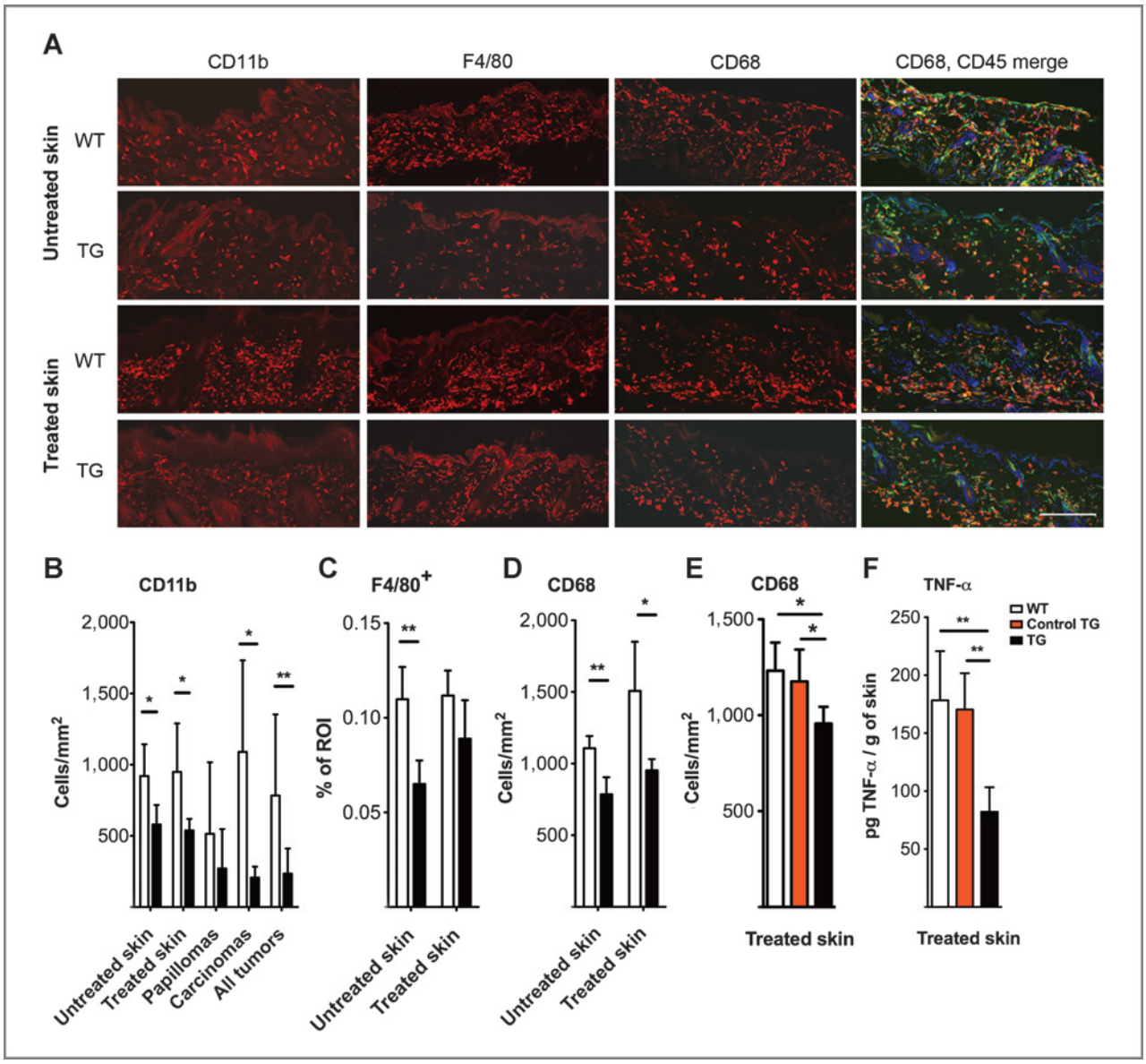

Figure 5. Analysis of macrophages in skin and tumors. A, untreated abdominal skin and DMBA-TPA–treated back skin stained for CD11b, F4/80, CD68, and CD45. Scale bar, 100 μm, Hoechst nuclear staining in blue. A significant portion of $CD45^+$ leukocytes are $CD68^+$ macrophages. B, quantification of $CD11b^+$ cells. Significant reduction of macrophage numbers in skin and carcinomas of transgenic mice, and a similar trend in papillomas. C, quantification of the area covered by $F4/80^+$ cells. D, density of $CD68^+$ cells in the skin. E, CD68 cell densities in DMBA-TPA–treated skin of wild-type, control transgenic, and transgenic mice. F, quantification of TNF-α expression in DMBA-TPA–treated skin of wild-type, control transgenic, and transgenic mice. Scale bar, 100 μm. $n = 4$–6; *, $P < 0.05$; **, $P < 0.01$.

lymph nodes, where they induce acquired immune responses. In addition, soluble antigens drained to the lymph nodes by the lymphatic vessels are taken up by lymph node–resident B cells and APCs for mounting of an acquired immune response. A chronic immune response may establish a protumorigenic tissue microenvironment and augment squamous tumor growth in the skin.

In the multistep chemical carcinogenesis SCC model used here, tumor growth is initiated by topical application of DMBA and promoted by weekly topical application of TPA, which induces epigenetic changes, inflammation, and hyperproliferation of basal keratinocytes (27). Simultaneously, the transcription of TNF-α is upregulated (28) and activates the classical signs of inflammation, including redness (blood vessel dilatation) and swelling (increased blood vascular permeability), resulting in continuous recruitment of inflammatory cells to the treated skin (27). After only three applications of TPA, the skin of transgenic mice seemed less inflamed than the skin of similarly treated wild-type mice. This led us to investigate potential changes in cutaneous inflammation following VEGFR-3 ligand blockage, as a possible reason for reduced tumor development and growth in the transgenic mice. Indeed,

Published OnlineFirst May 21, 2013; DOI: 10.1158/0008-5472.CAN-12-4539

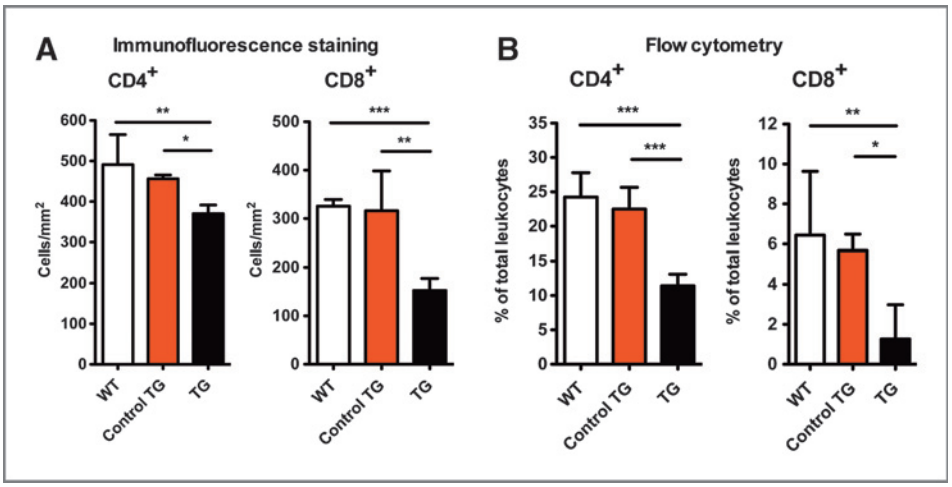

Figure 6. Quantification of CD45$^+$, CD4$^+$, and CD45$^+$, CD8$^+$ T cells in DMBA-TPA–treated skin. A, analysis of immunofluorescence staining. CD4, CD45 $n \geq 5$; CD8, CD45 $n \geq 4$. B, analysis by flow cytometry. $n = 5$–6, *, $P < 0.05$; **, $P < 0.01$; ***, $P < 0.001$.

in transgenic mice with VEGFR-3 ligand blockage, the densities of macrophages and T cells were reduced in untreated and DMBA-TPA–treated skin. This may be due to decreased antigen delivery to the skin draining lymph nodes in the sVEGFR-3 transgenic mice that have defective cutaneous lymphatic vessels. Because previous studies have shown that mice deficient of CD4$^+$ T cells have a decreased incidence of SCC (17), this suggests that the decreased inflammation, including fewer CD4$^+$ T cells, decreased the tumor growth promotion.

Because monocytes chemoattracted to tumor tissue produce angiogenic factors, monocyte and macrophage densities were studied in more detail. In contrast to the short-lived, so-called inflammatory monocytes, resident monocytes may give rise to the Tie2-expressing monocyte subset, which can potently promote tumor growth by secretion of angiogenic factors (29). The M2-activated subpopulation of tumor-associated macrophages may also express Tie2 (30). Despite a modest reduction of cell surface expression of Tie2 on transgenic macrophages and high IL-12 expression in DMBA-TPA–treated skin, no major differences were observed in the polarization of macrophages of wild-type and transgenic skin after the DMBA-TPA treatment. Thus, the mere reduction of macrophage density seen in the transgenic skin may account for the reduced tumor numbers.

Direct effects of VEGFR-3 ligand blockage are unlikely to explain for the reduced density of macrophages in the skin

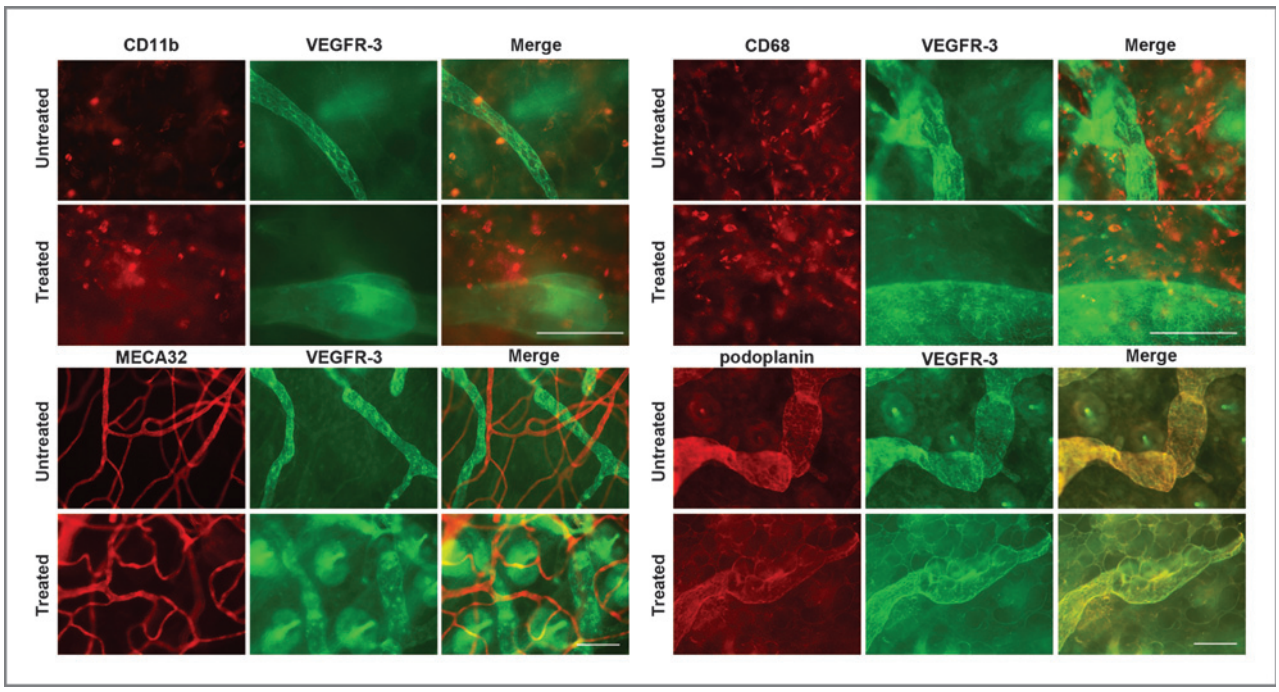

Figure 7. VEGFR-3 expression on cutaneous macrophages, lymphatic vessels, and blood vessels in wild-type mouse skin. Whole-mount staining of untreated or TPA-treated ear skin using antibodies against VEGFR-3, CD11b, CD68, MECA32, and podoplanin. Scale bars, 100 μm.

Published OnlineFirst May 21, 2013; DOI: 10.1158/0008-5472.CAN-12-4539

of the transgenic mice, because VEGFR-3 was not expressed by macrophages in untreated or DMBA-TPA–treated skin. VEGFR-3 expression in macrophages may depend on the tissue because expression was previously reported on macrophages in subcutaneously growing melanoma xenotransplants (10). Macrophage inflammatory protein 1α (MIP-1α) and MCP-1 (CCL2), important macrophage chemoattractants, were among the several macrophage-associated cytokines found at lower levels in the transgenic skin and in transgenic papillomas. The DMBA-TPA–induced inflammatory response includes elevated expression of MIP-1α (31), whereas MCP-1 is expressed by lymphatic endothelial cells (32). Thus, the lack of lymphatic vessels likely contributed to the reduced MCP-1 levels and reduced macrophage numbers in transgenic skin.

In contrast to the chemical carcinogenesis model used in this study, previously published studies on the blockage of VEGFR-3 signaling in cancer have used local injections of millions of tumor cells (7, 8, 33–36). This is quite different from the situation in human cancer. In particular, in tumor transplantation models, premalignant progression is circumvented by the selection and amplification of malignant cells in culture already before they are in contact with the tissue microenvironment. In contrast, in more than 20% of human cancers, inflammation may act as a critical promoter of tumor growth and progression (37). In the chemical carcinogenesis model, tumor growth requires a permissive tissue microenvironment, which is simulated by inflammation, induced by TPA. These features of the chemical carcinogenesis model allow the analysis of possible effects on early tumor growth in a cutaneous tissue microenvironment similar to the early development of NMSC in humans. To block VEGF-C and VEGF-D during more than 10 weeks of the chemical carcinogenesis treatment, we first tested viral gene delivery, but this failed to yield high sVEGFR-3 levels in the skin. We thus decided to use the constitutive K14/sVEGFR-3 transgenic model in which the sVEGFR-3 levels are upregulated by the carcinogenesis treatment, because of the increased expression of keratin14 by the hyperplastic epidermal keratinocytes. It would be of interest to investigate, in future studies, an inducible sVEGFR-3 transgene to restrict expression of the inhibitor to the carcinogenesis treatment period.

Because of the advantages of the chemical carcinogenesis model, we were able to show novel pleiotropic effects of VEGF-C and VEGF-D blockage in the tumor tissue microenvironment. Our new observations on inhibition of angiogenesis, blood vascular leakage, and the protumorigenic inflammatory tissue microenvironment support the use of VEGFR-3 ligand blockage not only to target tumor metastasis but also at early stages of tumor growth.

Disclosure of Potential Conflicts of Interest

No potential conflicts of interest were disclosed.

Authors' Contributions

Conception and design: A.K. Alitalo, M. Detmar
Development of methodology: A.K. Alitalo, S.T. Proulx, M. Detmar
Acquisition of data (provided animals, acquired and managed patients, provided facilities, etc.): A.K. Alitalo, S.T. Proulx, S. Karaman, D. Aebischer, S. Martino, M. Jost, N. Schneider, M. Bry
Analysis and interpretation of data (e.g., statistical analysis, biostatistics, computational analysis): A.K. Alitalo, S.T. Proulx, S. Karaman, D. Aebischer, S. Martino, M. Jost, N. Schneider, M. Bry, M. Detmar
Writing, review, and/or revision of the manuscript: A.K. Alitalo, S.T. Proulx, M. Detmar
Study supervision: M. Detmar

Acknowledgments

The authors thank Dr. P. Luciani and Prof. J.-C. Leroux for provision of near-infrared dyes, T. Laakkonen for help with the transgenic mouse line, and J. Scholl, F. Roudnicky, C. Ochoa, and H. Baumberger for technical assistance.

Grant Support

This work was supported by Swiss National Foundation grants 3100A0-108207 and 31003A-130627, Advanced European Research Council Grant LYVICAM, Krebsliga Schweiz, and Krebsliga Zurich (to M. Detmar).

The costs of publication of this article were defrayed in part by the payment of page charges. This article must therefore be hereby marked *advertisement* in accordance with 18 U.S.C. Section 1734 solely to indicate this fact.

Received December 12, 2012; revised April 8, 2013; accepted April 27, 2013; published OnlineFirst May 21, 2013.

References

1. Alitalo A, Detmar M. Interaction of tumor cells and lymphatic vessels in cancer progression. Oncogene 2012;31:4499–508.
2. Achen MG, Stacker SA. Vascular endothelial growth factor-D: signaling mechanisms, biology, and clinical relevance. Growth Factors 2012;30:283–96.
3. Tammela T, Zarkada G, Wallgard E, Murtomaki A, Suchting S, Wirzenius M, et al. Blocking VEGFR-3 suppresses angiogenic sprouting and vascular network formation. Nature 2008;454:656–60.
4. Tammela T, Zarkada G, Nurmi H, Jakobsson L, Heinolainen K, Tvorogov D, et al. VEGFR-3 controls tip to stalk conversion at vessel fusion sites by reinforcing Notch signalling. Nat Cell Biol 2011;13:1202–13.
5. Baldwin ME, Catimel B, Nice EC, Roufail S, Hall NE, Stenvers KL, et al. The specificity of receptor binding by vascular endothelial growth factor-d is different in mouse and man. J Biol Chem 2001;276:19166–71.
6. Hirakawa S, Brown LF, Kodama S, Paavonen K, Alitalo K, Detmar M. VEGF-C-induced lymphangiogenesis in sentinel lymph nodes promotes tumor metastasis to distant sites. Blood 2007;109:1010–7.
7. Karpanen T, Egeblad M, Karkkainen MJ, Kubo H, Yla-Herttuala S, Jaattela M, et al. Vascular endothelial growth factor C promotes tumor lymphangiogenesis and intralymphatic tumor growth. Cancer Res 2001;61:1786–90.
8. Laakkonen P, Waltari M, Holopainen T, Takahashi T, Pytowski B, Steiner P, et al. Vascular endothelial growth factor receptor 3 is involved in tumor angiogenesis and growth. Cancer Res 2007;67:593–9.
9. Mantovani A, Allavena P, Sica A, Balkwill F. Cancer-related inflammation. Nature 2008;454:436–44.
10. Skobe M, Hamberg LM, Hawighorst T, Schirner M, Wolf GL, Alitalo K, et al. Concurrent induction of lymphangiogenesis, angiogenesis, and macrophage recruitment by vascular endothelial growth factor-C in melanoma. Am J Pathol 2001;159:893–903.
11. Kerjaschki D, Regele HM, Moosberger I, Nagy-Bojarski K, Watschinger B, Soleiman A, et al. Lymphatic neoangiogenesis in human kidney transplants is associated with immunologically active lymphocytic infiltrates. J Am Soc Nephrol 2004;15:603–12.
12. Makinen T, Jussila L, Veikkola T, Karpanen T, Kettunen MI, Pulkkanen KJ, et al. Inhibition of lymphangiogenesis with resulting lymphedema in transgenic mice expressing soluble VEGF receptor-3. Nat Med 2001;7:199–205.

Published OnlineFirst May 21, 2013; DOI: 10.1158/0008-5472.CAN-12-4539

13. Hawighorst T, Velasco P, Streit M, Hong YK, Kyriakides TR, Brown LF, et al. Thrombospondin-2 plays a protective role in multistep carcinogenesis: a novel host anti-tumor defense mechanism. EMBO J 2001;20:2631–40.
14. Proulx ST, Luciani P, Alitalo A, Mumprecht V, Christiansen AJ, Huggenberger R, et al. Non-invasive dynamic near-infrared imaging and quantification of vascular leakage in vivo. Angiogenesis 2013 Jan 17. [Epub ahead of print]
15. Hirakawa S, Kodama S, Kunstfeld R, Kajiya K, Brown LF, Detmar M. VEGF-A induces tumor and sentinel lymph node lymphangiogenesis and promotes lymphatic metastasis. J Exp Med 2005;201:1089–99.
16. Holness CL, da Silva RP, Fawcett J, Gordon S, Simmons DL. Macrosialin, a mouse macrophage-restricted glycoprotein, is a member of the lamp/lgp family. J Biol Chem 1993;268:9661–6.
17. Daniel D, Meyer-Morse N, Bergsland EK, Dehne K, Coussens LM, Hanahan D. Immune enhancement of skin carcinogenesis by CD4+ T cells. J Exp Med 2003;197:1017–28.
18. Sica A, Larghi P, Mancino A, Rubino L, Porta C, Totaro MG, et al. Macrophage polarization in tumour progression. Semin Cancer Biol 2008;18:349–55.
19. Benedito R, Rocha SF, Woeste M, Zamykal M, Radtke F, Casanovas O, et al. Notch-dependent VEGFR3 upregulation allows angiogenesis without VEGF-VEGFR2 signalling. Nature 2012;484:110–4.
20. Moussai D, Mitsui H, Pettersen JS, Pierson KC, Shah KR, Suarez-Farinas M, et al. The human cutaneous squamous cell carcinoma microenvironment is characterized by increased lymphatic density and enhanced expression of macrophage-derived VEGF-C. J Invest Dermatol 2011;131:229–36.
21. Sauter ER, Nesbit M, Watson JC, Klein-Szanto A, Litwin S, Herlyn M. Vascular endothelial growth factor is a marker of tumor invasion and metastasis in squamous cell carcinomas of the head and neck. Clin Cancer Res 1999;5:775–82.
22. Nilsson I, Bahram F, Li X, Gualandi L, Koch S, Jarvius M, et al. VEGF receptor 2/-3 heterodimers detected *in situ* by proximity ligation on angiogenic sprouts. EMBO J 2010;29:1377–88.
23. Joukov V, Sorsa T, Kumar V, Jeltsch M, Claesson-Welsh L, Cao Y, et al. Proteolytic processing regulates receptor specificity and activity of VEGF-C. EMBO J 1997;16:3898–911.
24. Saaristo A, Veikkola T, Enholm B, Hytonen M, Arola J, Pajusola K, et al. Adenoviral VEGF-C overexpression induces blood vessel enlargement, tortuosity, and leakiness but no sprouting angiogenesis in the skin or mucous membranes. FASEB J 2002;16:1041–9.
25. Mkonyi LE, Bletsa A, Fristad I, Wiig H, Berggreen E. Importance of lymph vessels in the transcapillary fluid balance in the gingiva studied in a transgenic mouse model. Am J Physiol Heart Circ Physiol 2010; 299:H275–83.
26. Nagy JA, Benjamin L, Zeng H, Dvorak AM, Dvorak HF. Vascular permeability, vascular hyperpermeability and angiogenesis. Angiogenesis 2008;11:109–19.
27. Mueller MM. Inflammation in epithelial skin tumours: old stories and new ideas. Eur J Cancer 2006;42:735–44.
28. Verma AK, Wheeler DL, Aziz MH, Manoharan H. Protein kinase Cepsilon and development of squamous cell carcinoma, the nonmelanoma human skin cancer. Mol Carcinog 2006;45:381–8.
29. Coffelt SB, Lewis CE, Naldini L, Brown JM, Ferrara N, De Palma M. Elusive identities and overlapping phenotypes of proangiogenic myeloid cells in tumors. Am J Pathol 2010;176:1564–76.
30. De Palma M, Venneri MA, Galli R, Sergi L, Politi LS, Sampaolesi M, et al. Tie2 identifies a hematopoietic lineage of proangiogenic monocytes required for tumor vessel formation and a mesenchymal population of pericyte progenitors. Cancer Cell 2005;8:211–26.
31. Cataisson C, Joseloff E, Murillas R, Wang A, Atwell C, Torgerson S, et al. Activation of cutaneous protein kinase C alpha induces keratinocyte apoptosis and intraepidermal inflammation by independent signaling pathways. J Immunol 2003;171:2703–13.
32. Mancardi S, Vecile E, Dusetti N, Calvo E, Stanta G, Burrone OR, et al. Evidence of CXC, CC and C chemokine production by lymphatic endothelial cells. Immunology 2003;108:523–30.
33. Lin J, Lalani AS, Harding TC, Gonzalez M, Wu WW, Luan B, et al. Inhibition of lymphogenous metastasis using adeno-associated virus-mediated gene transfer of a soluble VEGFR-3 decoy receptor. Cancer Res 2005;65:6901–9.
34. He Y, Kozaki K, Karpanen T, Koshikawa K, Yla-Herttuala S, Takahashi T, et al. Suppression of tumor lymphangiogenesis and lymph node metastasis by blocking vascular endothelial growth factor receptor 3 signaling. J Natl Cancer Inst 2002;94:819–25.
35. He Y, Rajantie I, Pajusola K, Jeltsch M, Holopainen T, Yla-Herttuala S, et al. Vascular endothelial cell growth factor receptor 3-mediated activation of lymphatic endothelium is crucial for tumor cell entry and spread via lymphatic vessels. Cancer Res 2005; 65:4739–46.
36. Krishnan J, Kirkin V, Steffen A, Hegen M, Weih D, Tomarev S, et al. Differential in vivo and in vitro expression of vascular endothelial growth factor (VEGF)-C and VEGF-D in tumors and its relationship to lymphatic metastasis in immunocompetent rats. Cancer Res 2003; 63:713–22.
37. Ben-Neriah Y, Karin M. Inflammation meets cancer, with NF-kappaB as the matchmaker. Nat Immunol 2011;12:715–23.

Cancer Research
The Journal of Cancer Research (1916–1930) | The American Journal of Cancer (1931–1940)

AACR American Association for Cancer Research

VEGF-C and VEGF-D Blockade Inhibits Inflammatory Skin Carcinogenesis

Annamari K. Alitalo, Steven T. Proulx, Sinem Karaman, et al.

Cancer Res Published OnlineFirst May 21, 2013.